A Potential Role for the Gsdf–eEF1α Complex in Inhibiting Germ Cell Proliferation: A Protein-Interaction Analysis in Medaka (*Oryzias latipes*) From a Proteomics Perspective

Authors

Xinting Zhang, Yuyang Chang, Wanying Zhai, Feng Qian, Yingqing Zhang, Shumei Xu, Haiyan Guo, Siyu Wang, Ruiqin Hu, Xiaozhu Zhong, Xiaomiao Zhao, Liangbiao Chen, and Guijun Guan

Correspondence

lbchen@shou.edu.cn; gjguan@shou.edu.cn

Graphical Abstract

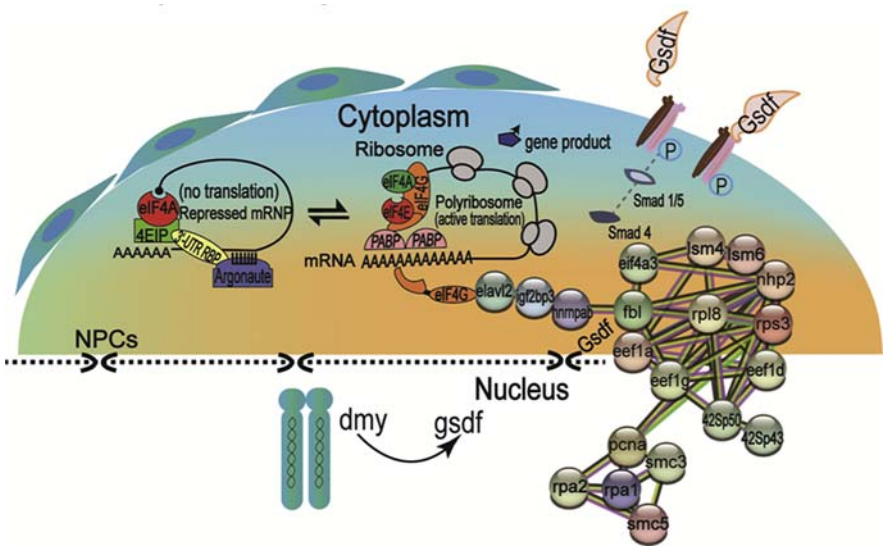

In Brief

gsdf is a unique TGFα essential for testicular differentiation in medaka *(Oryzias latipes).* We used a His-tag "pull-down" assay and a yeast 2-hybrid (Y2H) screening to identify a Gsdf–eEF1α complex in the adult testis. Physical interaction of Gsdf and eEF1α was confirmed by a paired Y2H assay and coimmunoprecipitation in the adult testis. Results of proteomics analysis (PXD022153) and ultrastructural observations support the potential role of the Gsdf–eEF1α complex in inhibiting germ cell proliferation, which may be conserved in vertebrates.

Highlights

- The Gsdf–eEF1α complex is essential for testicular development in the medaka.
- Gsdf inhibits female-specific protein synthesis *via* the Gsdf–eEF1α complex.
- Loss of Gsdf leads to the mitochondrial abnormality.
- The absence of Gsdf-eEF1α-actin complex in *gsdf* deficiency leads to the formation of male nucleus and female cytoplasmic dysgenesis germ cells.

2021, Mol Cell Proteomics *20*, 100023

https://doi.org/10.1074/mcp.RA120.002306

A Potential Role for the Gsdf–eEF1α Complex in Inhibiting Germ Cell Proliferation: A Protein-Interaction Analysis in Medaka (*Oryzias latipes*) From a Proteomics Perspective

Xinting Zhang[1,2,3,‡], Yuyang Chang[1,2,3,‡], Wanying Zhai[1,2,3,‡], Feng Qian[4], Yingqing Zhang[1,2,3], Shumei Xu[1,2,3], Haiyan Guo[1,2,3], Siyu Wang[1,2,3], Ruiqin Hu[1,2,3], Xiaozhu Zhong[5], Xiaomiao Zhao[5], Liangbiao Chen[1,2,3,*], and Guijun Guan[1,2,3,*]

Gonadal soma–derived factor (*gsdf*) has been demonstrated to be essential for testicular differentiation in medaka (*Oryzias latipes*). To understand the protein dynamics of Gsdf in spermatogenesis regulation, we used a His-tag "pull-down" assay coupled with shotgun LC-MS/MS to identify a group of potential interacting partners for Gsdf, which included cytoplasmic dynein light chain 2, eukaryotic polypeptide elongation factor 1 alpha (eEF1α), and actin filaments in the mature medaka testis. As for the interaction with transforming growth factor β–dynein being critical for spermatogonial division in *Drosophila melanogaster*, the physical interactions of Gsdf–dynein and Gsdf–eEF1α were identified through a yeast 2-hybrid screening of an adult testis cDNA library using Gsdf as bait, which were verified by a paired yeast 2-hybrid assay. Coimmunoprecipitation of Gsdf and eEF1α was defined in adult testes as supporting the requirement of a Gsdf and eEF1α interaction in testis development. Proteomics analysis (data are available *via* ProteomeXchange with identifier PXD022153) and ultrastructural observations showed that Gsdf deficiency activated eEF1α-mediated protein synthesis and ribosomal biogenesis, which in turn led to the differentiation of undifferentiated germ cells. Thus, our results provide a framework and new insight into the coordination of a Gsdf (transforming growth factor β) and eEF1α complex in the basic processes of germ cell proliferation, transcriptional and translational control of sexual RNA, which may be fundamentally conserved across the phyla during sexual differentiation.

Members of the transforming growth factor β (TGFβ) family are essential for the cooperation between somatic cells and germ cells during gametogenesis in vertebrates (1). The TGFβ is found across various species in spite of its functional diversity, such as the maintenance of the primordial follicle pool in mouse ovaries (2), keeping germ stem cells undifferentiated and regulating germ stem cell proliferation in *Drosophila* spermatogenesis (3), and association with follicular atresia in *Caenorhabditis elegans* and rats (4, 5). Gonadal soma–derived factor (*gsdf*), a unique TGFβ, has been demonstrated to promote the proliferation of type A spermatogonia at the mRNA and protein levels in rainbow trout testes (6). However, hypertrophic gonads with excessive germ cell proliferation were developed in *gdsf* KO (*gsdf* KO) medaka (*Oryzias latipes*), zebrafish (*Danio rerio*), and Nile tilapia (*Oreochromis niloticus*) (7–10), indicating that the comprehensive response of germ cells to Gsdf remains to be elucidated.

In medaka, *gsdf* has been demonstrated to be involved in a somatic male pathway under *dmy/dmrt1bY* regulation (a Y-specific DM-domain gene) (11, 12). However, germ cells autonomously adopt their own sexual fates through intrinsic *foxl3* (forkhead box L3), which has been shown by the evidence of fertile sperm development within a functional ovary after targeted disruption of *foxl3* (13). The sexually dimorphic expression of *sdgc* (sex determination in germ cells) occurs earlier than *dmy/dmrt1bY* somatic expression and is highly enriched in undifferentiated XY germ cells before the gonadal primordium is formed (14). Germ cells have a feminizing effect, which has been demonstrated by a series of XX mutants in different stages of gametogenesis (15), indicating that the identity of an XX germ cell is distinct from that of an XY germ cell. We have reported that two kinds of germ cells, those with positive or negative expression of Igf2bp3 and H3K27me3, were located in the same cyst of a *gsdf* KO XY ovary in the

From the [1]Key Laboratory of Freshwater Aquatic Genetic Resources, Ministry of Agriculture and Rural Affairs, Shanghai Ocean University, [2]International Research Center for Marine Biosciences, Ministry of Science and Technology, Shanghai Ocean University, [3]Key Laboratory of Exploration and Utilization of Aquatic Genetic Resources, Ministry of Education, Shanghai Ocean University, Shanghai, China; [4]Shanghai Genomics, Inc, Shanghai, China; [5]Department of Obstetrics and Gynecology, Sun Yat-sen Memorial Hospital, Sun Yat-sen University, Guangdong, China

‡These authors contributed equally to this work.

*For correspondence: Liangbiao Chen, lbchen@shou.edu.cn; Guijun Guan, gjguan@shou.edu.cn.

https://doi.org/10.1074/mcp.RA120.002306

early pachytene stage of meiosis I, but not in normal XX ovaries or normal XY testes (16). These results suggest that XY germ cells may have become heterogeneous in response to a Gsdf signal because of incomplete mitotic division.

It was reported that the impairment of anti–Müllerian hormone receptor 2 (*amhr2*, hotei mutant) resulted in half-hypertrophic XY ovaries and half-hypertrophic XY testes, and 1/10 of the gonads in XY hotei homozygotes were ovotestes, which contained testicular and ovarian components in one gonad (17, 18). Because Gsdf and Amh share a common TGFβ domain at the C-terminus, both *hotei* and *gsdf* mutants undergo XY sex reversal and exhibit a similar germ cell overproliferation phenotype (8, 18), which led us to speculate that Gsdf might act as a potential ligand to compete with Amh for Amhr2 binding to regulate the proliferation and differentiation of germ cells in medaka. To explore the potential role of Gsdf, including its synergistic effect with other TGFβs on somatic and germ cell differentiation, we used three approaches: a His-tag "pull-down" assay coupled with shotgun LC-MS/MS to identify the interactive partners for Gsdf, a Y2H screening using full-length Gsdf as bait to identify a group of potential interaction partners for Gsdf, and a comparison of proteomics profiles among adult gonads of normal and *gsdf* mutant medaka.

EXPERIMENTAL PROCEDURES

Animals

The medaka strains Hd-rR (*O. latipes*), HNI-II (*Oryzias sakaizumii*), and *dmy* mutant XY^{wOur} (MT206) provided by the National BioResource Project (https://www.shigen.nig.ac.jp/medaka/) were housed in recirculating systems at 26 to 28 °C, with a light–dark cycle of 14 h of daylight and 10 h of darkness and handled in strict compliance with the guidance of the Committee for Laboratory Animal Research in Shanghai Ocean University. Phenotypic sex was assessed according to the dorsal and anal fin shape and confirmed by gonadal biopsy. Genotyping of *dmy* and *gsdf* was performed using proper primer sets listed in supplemental Table S1 (8, 12).

Generation of Transgenic Intersex Medaka

A transgenic medaka was generated through a modification of original mγF-cry-EGFP (p817-EGFP, Addgene Plasmid 23156, constructed by Dr Kozmik), which contains a 271-bp mouse mγF-cry promoter–driving GFP reporter in the lens to facilitate preselection of transgenic medaka (19). GFP was replaced with the fragment of gsdf2AGFP (p817-gsdf2AGFP), which effectively caused XX male development *via* the ubiquitous expression under medaka β-actin promoter regulation (8). Next, 40 ng/μl of either plasmid DNA (p817-gsdf2AGFP) or control (p817-GFP) was used for pronuclear microinjection into fertilized eggs of HdrR-strain fish in the one-cell stage. Cells expressed GFP and Gsdf simultaneously because of the presence of gsdf2AGFP (Tg:gsdf). The transgenic lines were established by crossing the WT fish with the founder fish that could transfer GFP fluorescence to the offspring. The genotype analysis of the Sissy progeny is shown in Table 1, and details of Sissy generation are listed in supplemental Tables S2 and S3.

Table 1
Genotyping analysis of hybrid progenies (Tg $gsdf^{+/-}$XY♂ mating $gsdf^{-/-}$ XX ♀)

Offsprings	Heterozygotes (Ht, $gsdf^{+/-}$)		Homozygotes (Hm, $gsdf^{-/-}$)		Ht:Hm
	Tg+	Tg-	Tg+	Tg-	
XX	7♂	10♀	8♀	5♀	17:13
XY	5♂	9♂	11⚥	6♀	14:17
XX:XY	7:5	10:9	8:11	5:6	31:30

Histological and Ultrastructural Observation of Different Testes by Light and Transmission Electron Microscopes

Gonads were fixed in 4% paraformaldehyde solution, embedded in paraffin (Shenggong Co, Ltd), and cross sections were cut at 5-μm thickness for H&E staining as previously described (20). Small blocks of various testes were fixed in a mixture of 2.5% (v/v) glutaraldehyde in PBS (4 °C, pH 7.4, 0.1 M), overnight, postfixed in 1% (w/v) osmium tetroxide PBS for 1 h at RT, dehydrated in a graded ethanol series, and embedded in Epon 812. Ultrathin sections of 70-nm thickness were prepared using diamond knives on Leica EM UC7 Ultramicrotome, stained with 2% uranyl acetate (Merck, Darmstadt, Germany) and 2.8% lead citrate for 10 min per step, and examined with a FEI Tecnai G2 Spirit transmission electron microscope (Thermo Fisher) at an accelerating voltage of 30 kV.

His-tag Pull-Down Assay and MS Analysis

Escherichia coli strain C600 cells were transformed with a pET-32a plasmid containing a medaka gsdf ORF. The bacterial cells were grown in the LH medium containing 50 μg/ml of ampicillin at 37 °C, and the protein expression was induced by IPTG at a final concentration of 0.1 mM. The His–Gsdf fusion protein and His-tag protein were purified using anti-His beads (MBL Nagoya, Japan) following the manufacturer's instructions. Beads with bound His-tag protein were incubated with crude lysates from brains, ovaries, or testes pooled from 3 to 5 individuals as a single biologic sample, overnight on a roller at 4 °C and resolved using 10% SDS-PAGE. His–Gsdf fused proteins were purified with anti–His-tag antibody, visualized with Coomassie Brilliant Blue, and further verified by anti-Gsdf antibody. Gels in lanes containing His–Gsdf fused protein were excised, destained, and digested with trypsin. The peptide mixtures were extracted three times with 60% acetonitrile (Sigma-Aldrich Co)/0.1% TFA (Promega Co), and then pooled and dried completely by vacuum centrifugation for further identification using LC-MS/MS, according to the reported protocol (21).

Y2H Assay and cDNA Screening

The Y2H assay was performed to screen the potential components of the Gsdf-binding complex (22). A cDNA encoding Gsdf ORF without the signal peptide (1–19aa) was subcloned into a pGBKT7 vector (Matchmaker Two-Hybrid System 3; Clontech) to form a bait construct (pGB-Gsdf-1), in frame with the 3' end of the GAL4 DNA-BD to construct a fusion protein using an In-Fusion HD Cloning kit (Clontech). Next, mRNAs from adult testes were reverse-transcribed to cDNAs and subsequently fused to the pACT2 AD vector to form a pACT-cDNA prey library. Both bait and prey constructs were cocultured in 100 μl of the SD-Leu-Trp-His-Ade medium under drug selection. Only positive interactions from both bait and prey survived the Y2H screening system according to previous authors (23).

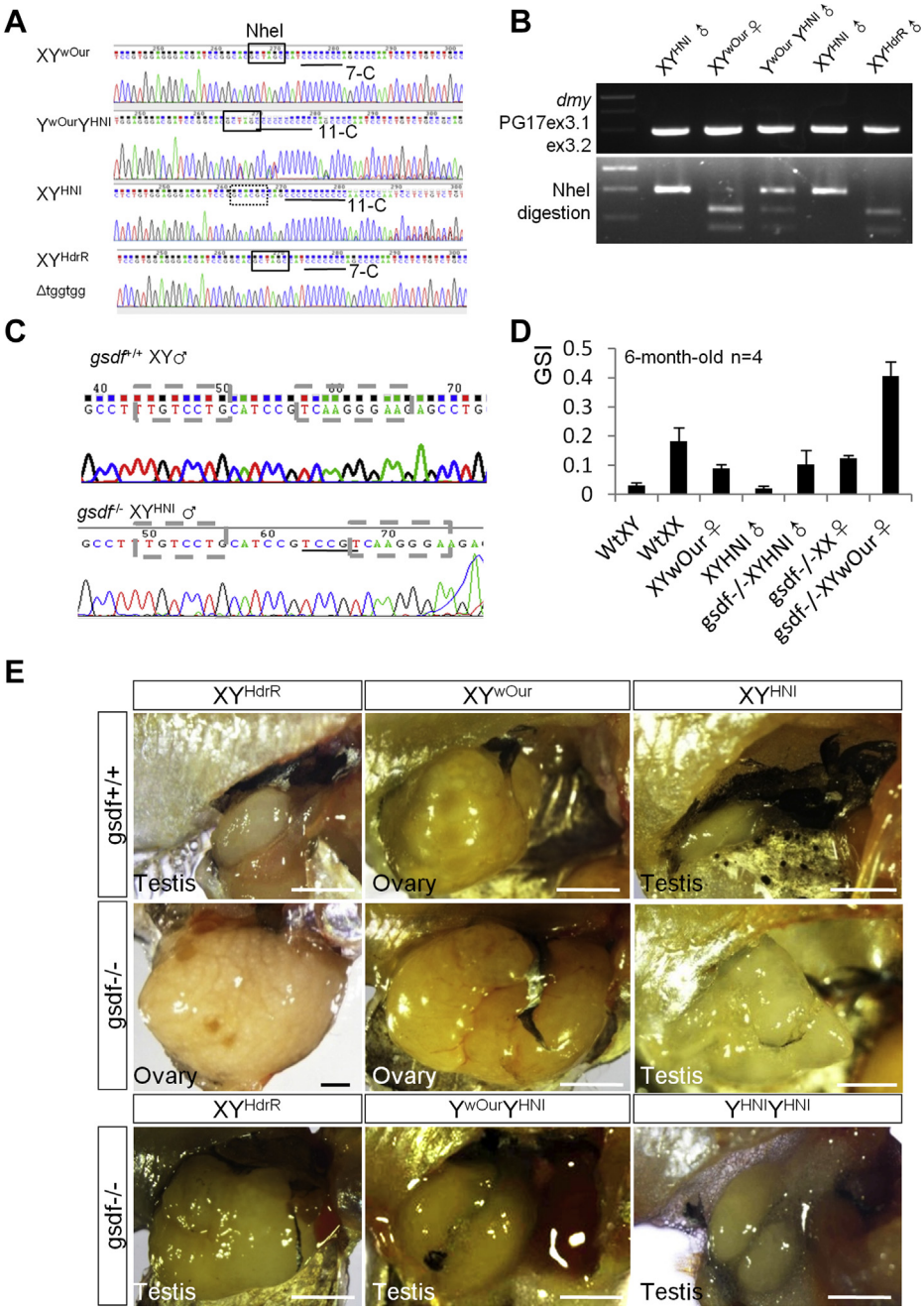

FIG. 1. **Gonad phenotypes of normal and gsdf mutant in variant dmy lines.** *A*, sequence analysis reveals variant dmy genes in Y^{wOur}, Y^{HNI}, and Y^{HdrR}. *B*, distinct RFLPs (restriction fragment length of polymorphism) in dmy exon 3 which can be recognized by specific primer set and NheI restriction enzyme. *C*, a normal XY male with intact gsdf, in contrast to gsdf mutants with four base-pair insertion in exon 2. *D*, the gonad-somatic index (GSI: the ratio of gonad weight to body weight) is highest in XY^{wOur} females based on measurements from at least 4 fish (6 months old) in each group. *E*, adult gonad morphologies of each line. Scale bar: 1 mm.

Label-Free Proteomic Analysis

Mature gonads of WT XX females, XY males, *gsdf*-deficient XY females, and Sissy intersex were pooled as a single biologic sample per group to minimize the influence of individual variants. Label-free proteomic analysis was performed in biologic triplicates described previously (16). Briefly, enzyme specificity was set as trypsin, whereas a maximum of 2 missed cleavages were allowed. Mass tolerances for precursor ions were set to 20 ppm in the first search and 5 ppm in the main search, and the mass tolerance for fragment ions was set to 0.02 Da. Protein abundance among the samples was determined using label-free quantification, with the false discovery rate (calculated as N(decoy)*([N(decoy)+N(target)]) and the threshold set to <1%; expected ion score cut-off was set to <0.05 (95% confidence). Raw data

were converted to Mascot generic peak lists using the MaxQuant search engine (v.1.5.2.8). Tandem mass spectra were searched against the *O. latipes* sequence database (UP000001038, 26,094 entries) using Mascot 2.0 (Matrix Science, London, UK). Both peptide and protein identifications were filtered using a cutoff of 1% for the peptide false discovery rate. The minimal and maximal peptide lengths were set to 6 and 144 amino acids, respectively. Proteins containing more than 1 unique peptide were considered unique. Gene ontology annotation was performed using the DAVID classification tool. Cluster membership was visualized by a heat map using the "heatmap.2" function from the "gplots." Functional network analysis of the identified differentially expressed proteins (DEPs) was performed with STRING (version 8.3, http://string.embl.de/).

Western Blot Analysis and Coimmunoprecipitation

Gonadal proteins were separated on 10% SDS-PAGE and Western-blotted (WB) onto polyvinylidene difluoride membranes as described previously (16). All information on the primary antibodies is listed in supplemental Table S4.

Anti–His-tag purified the recombinant His–Gsdf fusion protein described previously; the fusion protein was then incubated with sonicated lysates of adult gonadal extracts (derived from 3 to 5 individual ovaries or testes) overnight at 4 °C. After washing with 1× PBS/0.01% Tween-20 three times, the protein-bound beads were resuspended in a mixture of 20 μl of the elution buffer and 20 μl of 2× SDS loading buffer and resolved using SDS-PAGE. After that, detection was performed using anti–eukaryotic polypeptide elongation factor 1 alpha (eEF1α) first and then anti-Gsdf on the same polyvinylidene difluoride membrane.

Experimental Replicates and Statistical Analysis

All of the experiments were repeated at least 3 times to validate the quantitative protein abundance. Paired comparisons were performed using Student's t test with probabilities of $^{*}p < 0.05$, $^{**}p < 0.01$, and $^{***}p < 0.001$.

RESULTS

Gonadal Diversity of gsdf Mutants

Reduced dmy expression (XY^{wOur}, Y chromosome derived from an Oura XY female) during sexual differentiation leads to XY^{wOur} ovary development (24). The genotype of the *dmy* gene derived from XY^{HdrR}, XY^{wOur}, or XY^{HNI} (HNI XY, *O. Sakaiizumi*) can be distinguished by the presence of the Nhe I site and 7/11-c polymorphism, or the tggtgg deletion at −210 bp upstream of exon 3 (Fig. 1, *A* and *B*) (12). Although gsdf KO fish showed full XY feminization in the early developmental stage (8, 10), one-tenth of XY^{HdrR} or two-thirds of XY^{HNI} adult gonads developed into testes (Fig. 1) (10). The *gsdf* KO testes were larger than those of normal XY males, as the highest gonad-somatic index (the ratio of the gonad weight to the body weight; the raw data listed in supplemental Table S5*A*) of XY^{wOur} *gsdf* KO females was almost double that of normal or XY^{HdrR} *gsdf* KO ovaries/testes (Fig. 1, *D* and *E*), which is in agreement with the morphologic observations of the XY^{wOur} *gsdf* KO ovary. These results suggest that *gsdf* is not indispensable in *dmy*-regulated spermatogenesis but a potential trigger for germ cell proliferation.

Diversity of Germ Cell Responding to Gsdf

A stable XX male transgenic line (Tg:cryG) was generated by replacing medaka β-actin promoter with mouse γF-crystallin promoter, which drives the expression of Gsdf2AGFP fusion protein in the lens and gonads (supplemental Fig. S1) we described previously (8). After two generations of mating between Tg:gsdf transgenic fish and *gsdf* heterozygotes, 11 Tg:cryG $gsdf^{-/-}$ XY fish were obtained (termed as Sissy). They were characterized by a male parallelogram-shaped anal fin, but the abdomen was enlarged, containing an ovotestis almost 10 times larger than normal XY or XX male testes (supplemental Table S5*B*), occasionally found in *hotei* mutants (18). The schematic representation of Sissy generation is shown in supplemental Fig. S1, while details are listed in Table 1 and supplemental Tables S3 and S4. Histological analysis showed that the gonads of Tg:cryG XX individuals were changed to normal testes rather than following normal ovary development (Fig. 2, *A'–A''* and *B'–B''*). Distinct from normal testes ordered from a distal to proximal direction, germ cells were disordered because of excessive proliferation in the gonads of gsdf KO XY^{HNI} (Fig. 2, *C'–C''*). All 11 Sissy medakas (100%) had gonads containing both ovarian and testicular components (Fig. 2, *D–D''*), reflecting the diversity of germ cell responding to Gsdf signal.

Proteomic Analysis of Normal and gsdf *KO Gonads*

The profiles of normal XX ovaries (A) or XY testes (B), *gsdf*-deficient XY ovaries (C), and Sissy ovotestes (D) were performed using label-free proteomic analysis (16). The DEPs of upregulated and downregulated proteins underwent pair-wise comparison, and the DEPs were functionally annotated at threshold levels of above 1.2-fold or below 1:1.2-fold differences in protein expression, of 1549 proteins that were identified in all three biological replicates and listed in supplemental Table S5. A group *versus* D group revealed a large fluctuation range of 134 upregulated and 323 downregulated DEPs (supplemental Fig. S2*A*), as well as abundance of ribosome protein *rpl7s* and *rpl27s*, but less cytoplasmic actin (supplemental Fig. S2*B*. Interestingly, Musashi family Khdrbs1 and eIF4a3 of Sissy ovotestis maintained a higher male-like style (supplemental Fig. S2*C*). These results indicate that although the ribosome assembly level of Sissy ovotestes is as high as that of normal ovaries, the cytoskeleton organization still follows a male style (supplemental Fig. S2, *B* and *C*), which is consistent with histological observation of the dispersion of the diplotene oocytes in Sissy ovotestes (Fig. 2*D*).

A novel R-based package namely clusterProfiler was applied to further identify the functional kyoto encyclopedia of genes and genome (KEGG) enrichment of these overlapped DEPs (Fig. 3*A*). Two subsets of the KEGG pathway enrichment are the bubble map displayed in Figure 3*B*, while the entire details are listed in supplemental Table S6. The biogenesis of

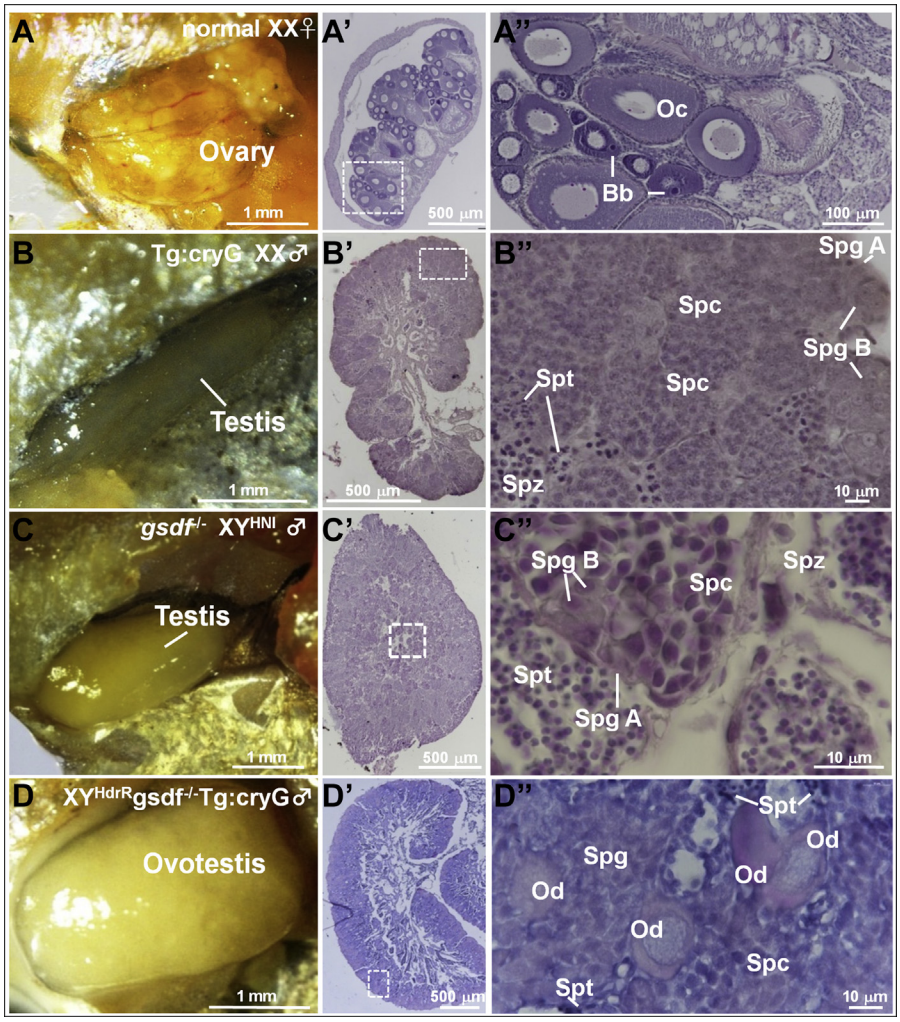

FIG. 2. **Different responses of XX and XY germ cells to Gsdf regulation.** Gonad morphology: *A*, normal XX ovary; *B*, Tg:cryG XX testis; *C*, gsdf $^{-/-}$XY^{HNI} hypertrophic testis; *D*, sissy ovotestis (Tg:cryG gsdf $^{-/-}$XY^{HdrR}) and histological cross-sections are *A*' to *D*', and enlarged images in *A*" to *D*". Both spermatogenesis and oogenesis coprogressing in ovotestis from Sissy gonad (*D*–*D*"). Bb, Balbiani body; *gsdf*, gonadal soma–derived factor; Oc, oocyte; Od, diplotene oocyte; Spc, spermatocyte; Spg, spermatogonia; Spt, spermatid; Spz, spermatozoa.

ribosomes was significantly enriched in the upregulated DEPs of A *versus* B and C *versus* B (Fig. 3*B*, 11 counts with the highest rich factor in supplemental Table S6). Thus, ribosome biogenesis was higher in normal and *gsdf* null ovaries but lower in normal testes, which is consistent with the quantity of ribosomes being actively transcribed and accumulated during early oogenesis (25, 26). In contrast, pathways of microtubule-based phagosomes and gap junctions, as well as cell cycle, represented by proliferating cell nuclear antigen, were enriched in B but downregulated in C and A, reflecting that these proteins are higher in normal testes than in normal ovaries or *gsdf*-deficient ovaries. It was noted that the levels of proteasome activator subunit 2 and proteasome 26S subunit, ATPase 2 (*psmc2*), were remarkably higher in normal testes and *gsdf*-deficient ovaries than in normal ovaries (Fig. 3*B*, supplemental Table S5), indicating that the proteasome regulatory switch of germ cell proliferation and meiosis entry found in *C. elegans* might still be active in *gsdf*-deficient ovaries (27).

To visualize changes between the intact and null *gsdf* mutant gonads, we further dissected predominant alterations in the abundance of 31 proteins using a Volcano plot in Figure 4*A*, and the bar plot to reflect the fold-changes relative to normal ovaries or testes in Figure 4*B*. Details of individual classifications and fold-changes in −10logP can be found in supplemental Table S7. Transcriptional RNA-binding factors (Elavl2, Igf2bp3, and 42Sp43) and translational elements (42Sp50) were dramatically activated in the ablation of *gsdf*, suggesting that Gsdf signaling may prevent the formation and storage of these 42S particles (Fig. 4, *A* and *B*). It was noted that eukaryotic Sm-like (Lsm) proteins (Lsm 4 and 6) (RNA-RNA chaperone essential for histone mRNA degradation) (28) were elevated in the *gsdf*-depleted ovary (Fig. 4 and supplemental Table S7), indicating that Gsdf signal potentially represses RNA degradation (including histone mRNA degradation) directly or indirectly. The structural maintenance of chromosomes 3 (SMC3) protein level in *gsdf*-deficient ovaries was lower than the level found in normal testes but higher than that of normal ovaries (Fig. 4*B*).

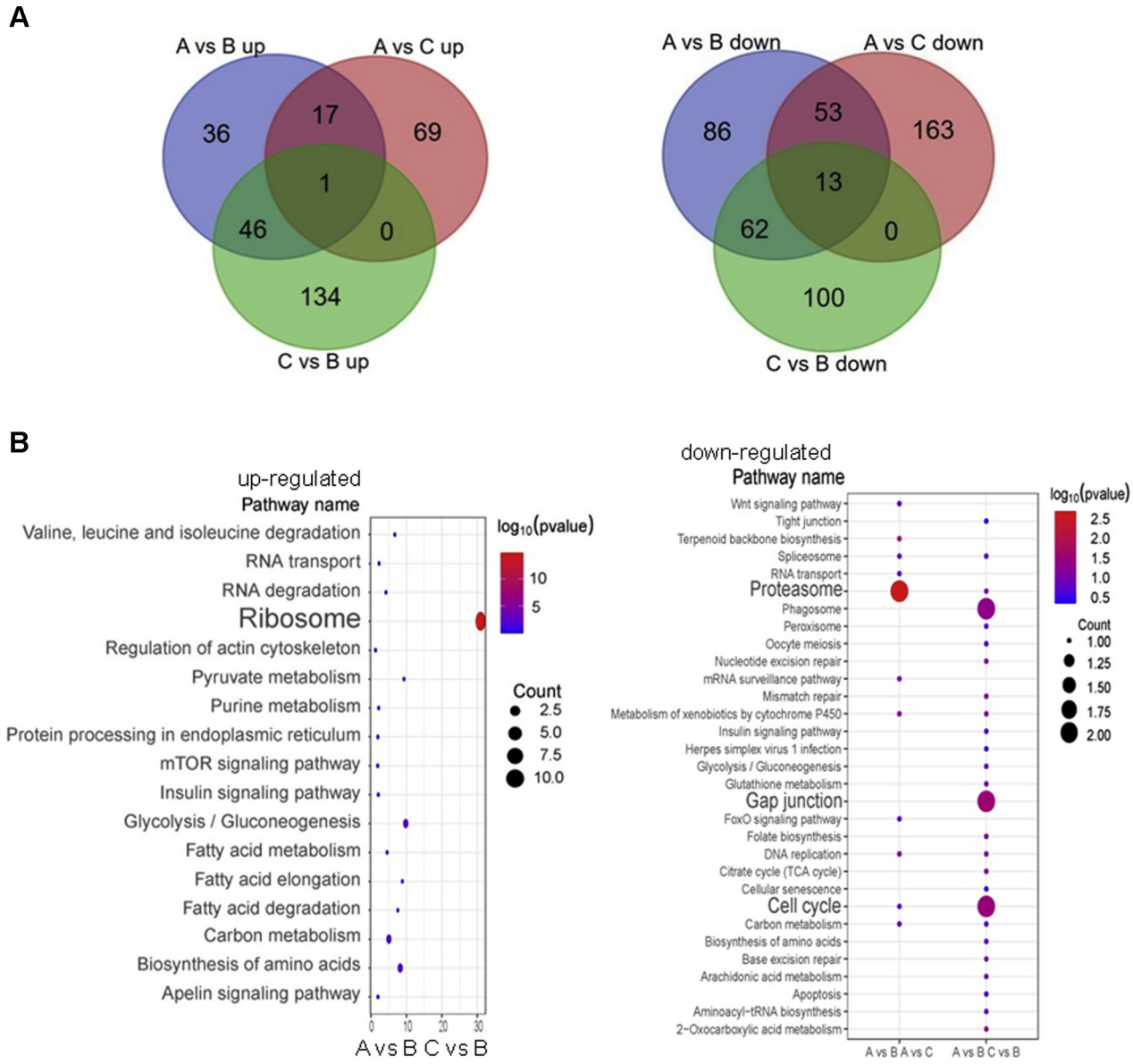

FIG. 3. **Robust protein expression under Gsdf regulation.** *A*, the Venn diagram shows the numbers of DEPs in upregulated or downregulated groups of A *versus* B, A/C, and C/B pairwise comparisons. *B*, the bubble plot depicts the enriched KEGG pathways in upregulated and downregulated groups using a novel R-based package, clusterProfiler. The *bubble*, with color ranging from *red* to *blue*, indicates a set of highly significant proteins. The diameter of the bubble indicates the number of genes related to the same KEGG pathway. A, normal ovaries; B, normal testes; C, gsdf KO XY ovaries. *gsdf*, gonadal soma–derived factor.

DEPs and KEGG pathway analysis showed that Gsdf signal transduction affected DNA replication, RNA metabolisms, vitellogenesis, and apoptosis through these upregulated and downregulated protein expressions.

Capture of Gsdf-Binding Protein by His-Tagged rGsdf Pull-Down Method

To identify the potential Gsdf-binding protein, we used His-tagged gsdf recombinant for pull-down analysis to capture the anti-His bead precipitation core protein complex of the adult testicular crude extract. This was then followed by mass spectrometric analysis. In addition, 50-kD and 25-kD fragments were detected in all input samples, which correspond to the heavy chain of mouse IgG and recombinant Gsdf, respectively. Only in the reaction of gsdf-intact normal testis extract can the band with a molecular weight greater than 100 kD be obtained (Fig. 5*A*). The band was further excised from our SDS-PAGE gel and subjected to MS analysis. The fractions of the protein complex are depicted as a pie chart in

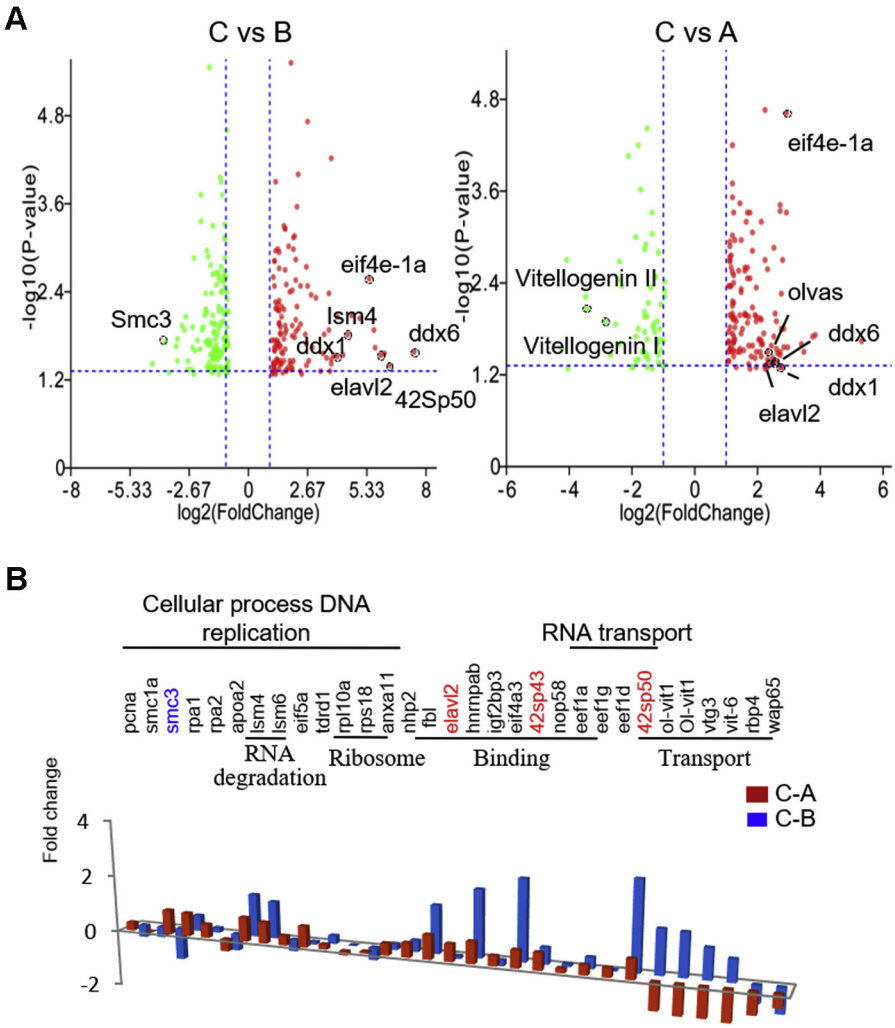

FIG. 4. **Significant DEPs upregulated and downregulated proteins by gsdf.** *A*, the Volcano plots of fold-change (FC) in protein abundance from gsdf KO ovary *versus* WT testis (C *versus* B) and C *versus* WT ovary (C *versus* A) are represented. Thresholds of FC ≥ 1.5 or FC ≤ −1.5 and significance (−10logP ≥ 1.5) are depicted by *dashed lines*. *B*, bar plots of FCs from C *versus* A and C *versus* B comparisons are represented in the Y-axis and classified by gene ontology in the same order as genes listed in supplemental Table S5. *gsdf*, gonadal soma–derived factor.

Figure 5*B*, and protein details are listed in supplemental Table S8. Forty-nine percent of the constituents were comprised of dynein light chain 1 (*dlc1*), followed by actin-β1 at 14%, and ribosomal proteins. It was reported that loss of dlc1 in the cyst cells caused gonial cell hyperplasia in *Drosophila* testes (29), resembling the phenotypes of germ cell overproliferation in *gsdf* depletion or *amhr2* mutation testes (8, 10, 18). In addition to ribosomal proteins, eukaryotic translation initiation factor 3 subunits, the structural maintenance of chromosomes 5, eEF1α, and its ovarian isoform (42Sp50), which are expressed in frog and medaka oocytes (25, 26), were found among the 36 identified peptides.

Physical Interaction Between eEF1α and Gsdf

To identify an interactive partner for Gsdf, we performed a Y2H assay using the full-length of Gsdf ORF as a bait plasmid and the prey plasmids encoding for proteins derived from the cDNAs of WT adult testes. Ultimately, 63 of the 66 colonies were recovered and sequenced. Gene annotation was performed and is listed in supplemental Table S9. eEF1α was captured twice from 63 sequenced clones (No. 27 and No. 72 in supplemental Table S9) and corresponded to different regions of eEF1α. Cytoplasmic dynein heavy chain 1 was also included in the core complex listed in supplemental Table S9.

We further performed coimmunoprecipitation to validate the interaction between eEF1α and Gsdf. Anti–His-tag antibody was used to purify fusion His-rGsdf after the incubation of gonadal lysates (*i.e.*, normal testis or ovary). A positive band of 100 kD was detected using anti-Gsdf as resolved by SDS-PAGE, further confirming the interaction of Gsdf and eEF1α (Fig. 5*C*). Anti-Gsdf or anti-eEF1α were able to detect endogenous Gsdf (75 kDa) and eEF1α (50 kDa), respectively (Fig. 5*C*).

Y2H pairing was carried out to verify the physical interaction between Gsdf and the putative binding factor. The membrane system was used with the bait plasmids PBT3-suc-acvr1, PBT3-suc-amhr2, PBT3-suc-tgfbr1, and PBT3-suc-tgfbr2, and the prey plasmid PPR3-N-Gsdf-1, which were

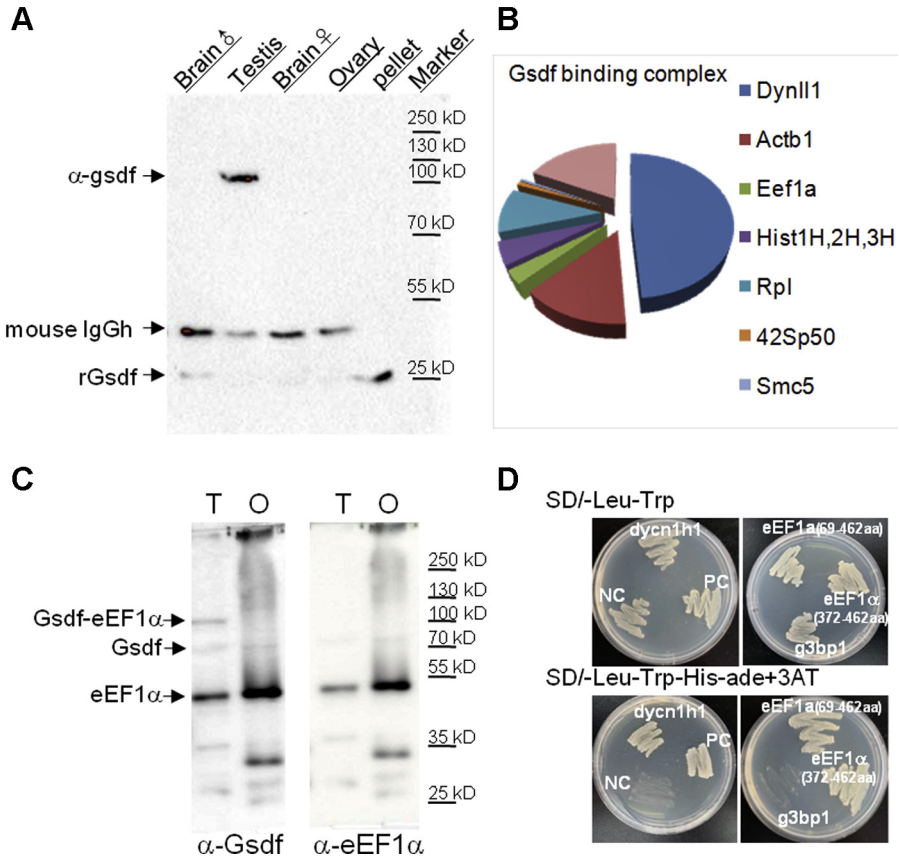

FIG. 5. **Isolation and identification of the Gsdf-binding complex.** *A*, His-tag-Gsdf recombinants were incubated with tissue lysates from male and female brains and gonads, pulled down using specific anti-His beads and separated with SDS-PAGE. The Gsdf-binding complex was detected with anti-Gsdf antibody and subjected to LC-MS/MS analysis. *B*, the pie chart represents the percentage of total protein abundance, and six principle components of the Gsdf-binding complex are listed on the *right*. Analytic details are provided in supplemental Table S1. *C*, the Gsdf–eEF1α complex was only detected in testis (T) extracts pulled down by anti-His beads, not detected in the ovary (O) by anti-Gsdf. *D*, physical binding of Gsdf, dyn1, and eEF1α demonstrated by Y2H. *gsdf*, gonadal soma–derived factor; rGsdf, recombinant Gsdf from a pET32-gsdf expression construct; Y2H, yeast 2-hybrid.

cotransformed into yeast strain NMY51 in alternating pairs. After confirming the absence of toxic effects and self-activation in selective plates, colony growth was observed in the cotransformation of prey and bait plasmids in selected plates (supplemental Fig. S3*A*). This indicated a potentially direct interaction between Gsdf and TGFβ/Activin/Amh receptors, consistent with the knowledge that TGFβ ligands are capable of binding to their cognate receptors during germ cell development and cross-reacting in mice (30). We further evaluated candidate partners for Gsdf interaction by Y2H assay. Among 13 examined colonies, seven demonstrated positive Gsdf interaction, as shown in Figure 5*D* and supplemental Fig. S3*B*. It was noteworthy that partial eEF1α (No. 72, 372-462aa, and No. 27, 69-462aa) interacted positively with Gsdf protein.

Transmission Electron Microscopic Observation of Mitochondrial Abnormality in gsdf KO Spermatogonia

Because Gsdf may interact with acetyl-CoA, the ultrastructural morphology of mitochondria in normal and *gsdf* KO spermatogonia was observed and compared. The spermatogonia and mitochondria in the testes of HdrR and HNI gsdf KO were larger than those of normal testes (Fig. 6), which was consistent with the significant activation of ribosomal biogenesis responsible for overproliferation in *gsdf* KO fish. Compared with the normal control group, *gsdf* KO mitochondria swelled, and the structure of tubular cristae was severely damaged (indicated by arrowheads in Fig. 7), suggesting that energy homeostasis and metabolism of *gsdf* KO spermatogonia were impaired, including ATP production.

Effect of gsdf on eEF1α-Mediated Cytoplasmic Protein Synthesis

The phosphorylation of Smads was detected in normal testes, weak in normal ovaries, and undetected in *gsdf* KO ovaries by WB using anti-Smad1/5-P antibody. The 142-kDa specific band against Smc3 was marked in normal testes and *gsdf* KO ovaries but weaker in normal ovaries (Fig. 8*A*), which is consistent with proteomic profiling analysis (Fig. 4*B*). The 125-kDa fragment of anti-acetyl Smc3 was only detectable in normal testes by WB (Fig. 8*A*), indicating that Smc3 was mainly deacetylated in gsdf KO ovaries. A network of 20 proteins was connected with paired relationships annotated with the STRING database, using the Markov Clustering Algorithm with inflation parameter 3 (Fig. 8*B*). Notably, in *gsdf*-deficient XY ovary, some networks showed ovarian expression patterns (including Igf2bp3, 42Sp50, and 42Sp43), whereas others were expressed more like patterns in the testis

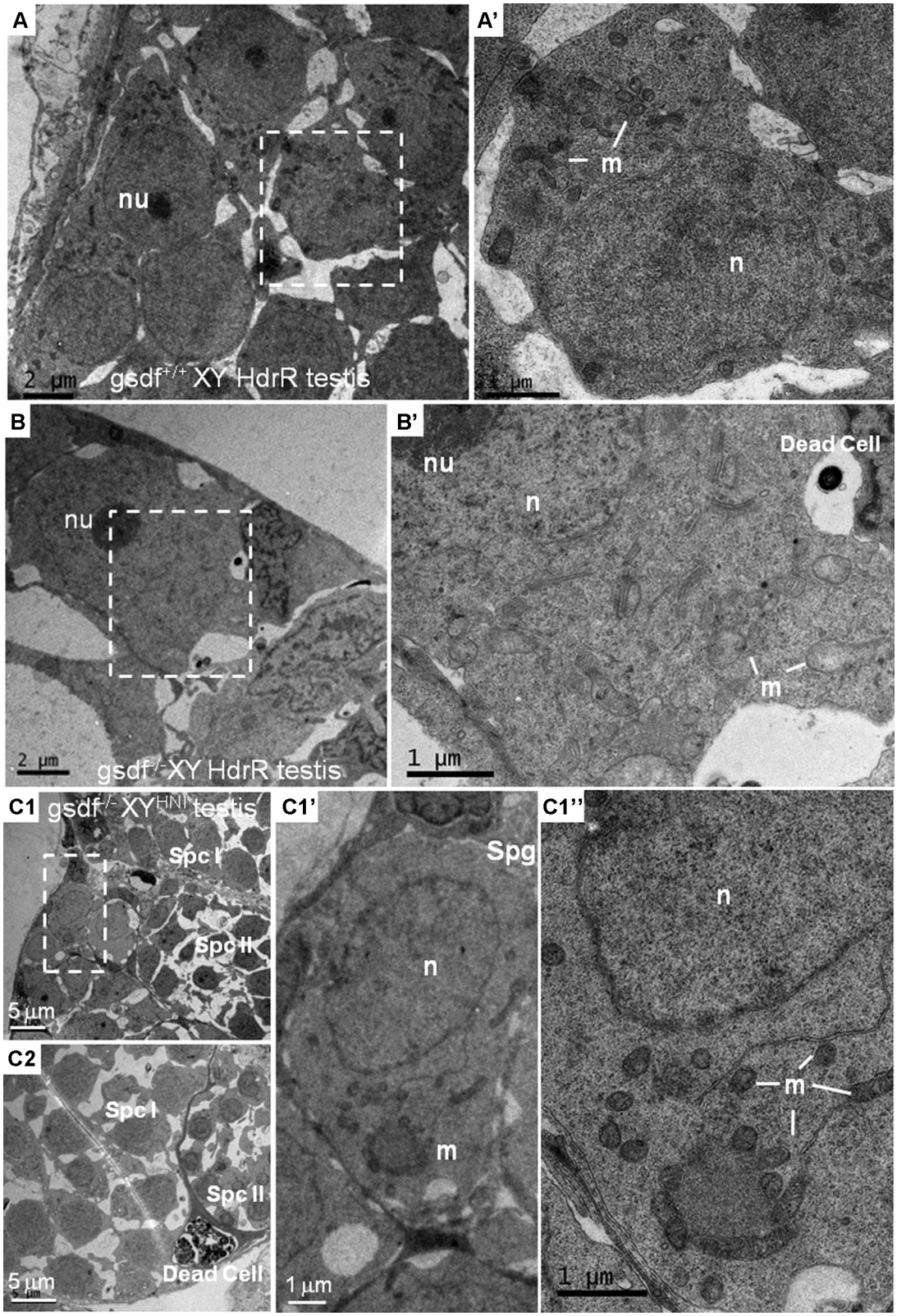

FIG. 6. **TEM images of ultrastructural details of various gonads.** *A*, the image in low magnification of normal HdrR XY testis (*A*); gsdf$^{-/-}$ HdrR XY testis (*B*); XY^{HNI} gsdf$^{-/-}$ testis (*C*); and high magnification (*A'*), (*B'*), and (*C1'–C1''*). Spermatogonia with nuclei surrounded by nuages and mitochondria. gsdf$^{-/-}$ spermatogonia and mitochondria are bigger than those of normal testes. Many dead cells were seen in *B* and *C*, but rarely in normal testes. Spg, spermatogia; SpcI, spermatocyte I; n, nucleus; nu, nucleolus; m, mitochondria; *gsdf*, gonadal soma–derived factor; TEM, transmission electron microscope.

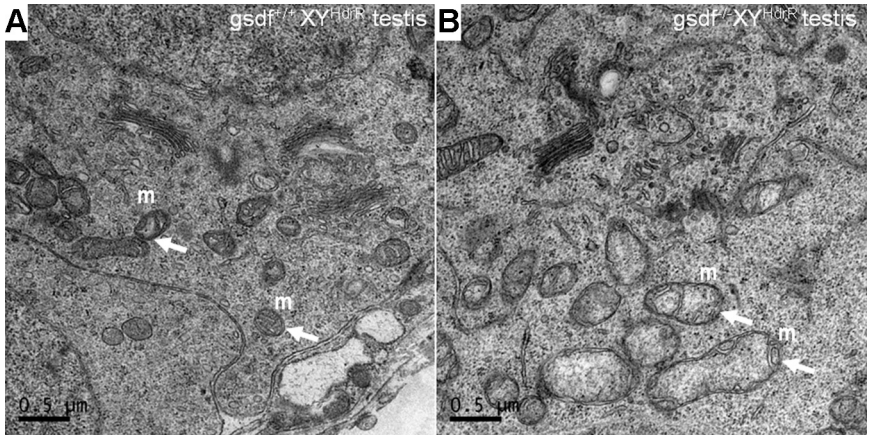

FIG. 7. **Mitochondrial abnormalities in gsdf KO spermatogonia.** *A*, images of normal HdrR XY testis (*A*) and XY gsdf−/− testis (*B*). m, mitochondria; *gsdf*, gonadal soma–derived factor.

(Smc3, slightly lower than the normal testis but significantly higher than the normal ovary) (Fig. 4), reflecting a distorted network that shares the complex cross-link force between male nucleus and female cytoplasm (Fig. 4*B*). Therefore, the loss of *gsdf* not only affects the signal transduction pathway for Tgfβ–Smad but also directly or indirectly affects the synthesis of proteins in the nucleus and cytoplasm through RNA transcription, RNA transportation, and/or RNA degradation mediated by eEF1α in germ cells (Fig. 8*B*) (16, 26).

DISCUSSION

Currently, the question of how germ cells transition from quiescence into self-renewal or sexual differentiation is still poorly known. Our findings link the mechanism of germ-cell proliferation and differentiation for vertebrates and invertebrates. Through pull-down assay and Y2H analysis, we confirmed that the Gsdf complex was composed of DLC1 and eEF1α. A similar phenotype of gonadal hyperplasia caused by *dlc1* mutation was shown in *Drosophila* testes (29), and the overproliferation in *gsdf* KO demonstrated that *dlc1* plays a conservative role in flies and fish. It has been reported that DLC1 is associated with human spermatogenesis (31). The Gsdf–eEF1α complex may directly or indirectly inhibit eEF1α-mediated protein synthesis, as the significant increase in eEF1α protein expression and ribosome activation was found in *gsdf* KO hypertrophic ovaries or testes compared with the low levels seen in normal ovaries and testes (Fig. 4 and supplemental Fig. S2). The remarked increase of eEF1α may overcome the downregulation effect from translational inhibitor Nanos2, which was demonstrated to partly participate in the translational quiescence of primordial germ cells (32). The lack of Gsdf–eEF1α–actin complex in gsdf KO may also lead to changes in the spatial structure of the cytoskeleton and affect the efficiency of protein synthesis, which eventually leads to protein synthesis in male nucleus and female ooplasm (Fig. 4*B*). This status of confused sex may further induce the transformation of eEF1α in a Yin-Yang type of effect from post-translation modification to protein degradation by activating the proteasome pathway (Fig. 3*B*) (33). Transgenic GFP fish revealed that eEF1α is universally expressed, whereas 42Sp50 is oocyte specific in medaka (26, 34) as one of the earliest markers of female sexual differentiation identified by a subtractive cDNA library screening in medaka (35). Both eEF1α and 42Sp50 protein levels were significantly increased in *gsdf* KO revealed by proteomics analysis (Fig. 4*B* and supplemental Fig. S2), while the physical interaction ability between Gsdf and 42Sp50 was verified by Y2H (date not published), suggesting that the transfer of Gsdf binding from eEF1α to 42Sp50 may play an important role in the transition of gametogenesis from spermatogenesis to oogenesis. In addition, Ddx6 and Elavl2, the RNA-binding proteins indispensable for the formation of quiescent primordial follicles in mice (36), were elevated in *gsdf*-deficient ovaries (Fig. 4). This is consistent with the accumulation of primordial follicles in the *gsdf* KO XY hypertrophic ovaries visualized by a multifluorescent GRY transgenic line in our previous report (37). The underlying mechanism(s), including the Gsdf–eEF1α complex direct inhibition of germ cell proliferation, needs to be addressed in future studies.

The unique Tgfβ family adapts to fewer receptors being stimulable to more ligands by combining the diversification of Tgfβ receptors and versatility of signaling responses (Smad-dependent and Smad-independent pathways) (38). Therefore, the binding ability of Gsdf to a variety of Tgfβ receptors (including Amhr2) as proved by the Y2H-pairing interaction was not unexpected. In this study, evidence of Gsdf binding to Amhr2, suggested that Gsdf and Amhr2 might be closely related as a pair of ligands and receptors, which could well explain some overlapping phenotypes of *gsdf* and *amhr2* mutants. The reason for the failure to isolate Tgfβ receptors by Y2H screening or His-tag pull-down analysis may be that the functional receptor needs to form tetramers to make Y2H undetectable or that the binding force between the ligand and receptor is too weak to be detected. The *gsdf* KO showed differential proportions of ovarian or testicular hyperplasia

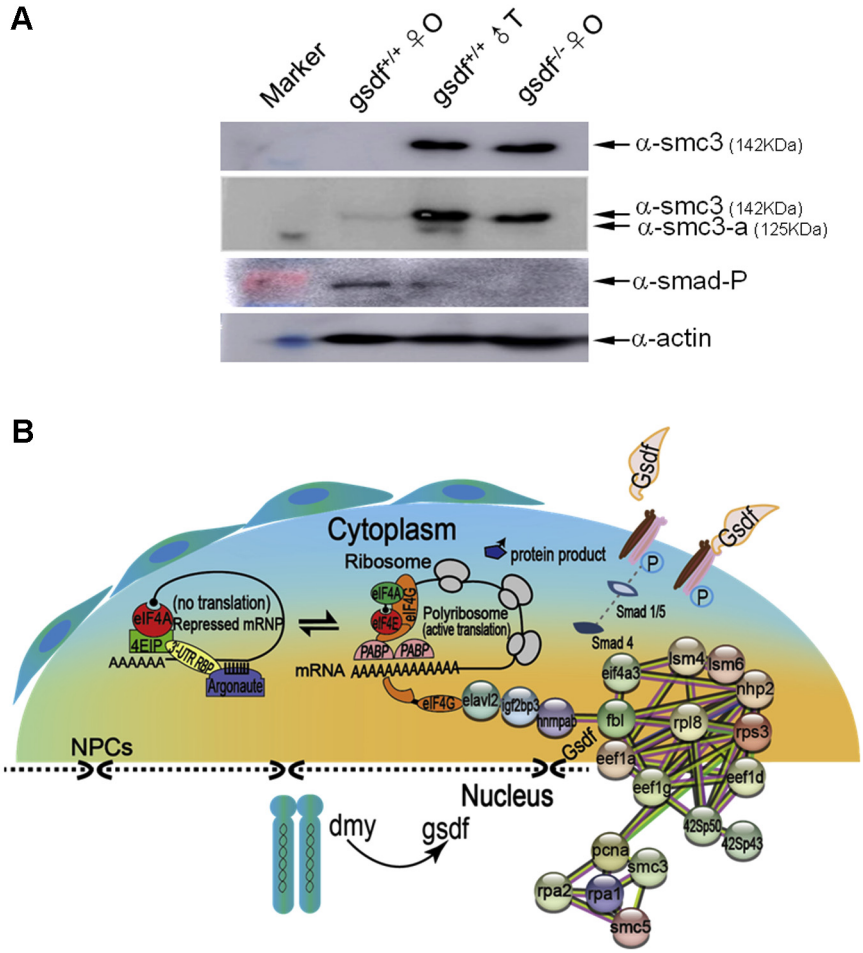

FIG. 8. **Protein dynamics under Gsdf regulation.** *A*, the conventional pathway of Smad phosphorylation under Gsdf–TGFβ receptor regulation. *B*, the schematic illustration of cellular machineries of protein translation under the regulation of the Gsdf-associated complex in germ cells. Gsdf–eEF1α impairment is accompanied by germ-cell transformation from spermatocytes into oocytes, an increase of female 42Sp50, and a decrease of Smad1/5 phosphorylation. The cytoplasmic protein network is predicted by STRING analysis. *gsdf*, gonadal soma–derived factor; TGFβ, transforming growth factor β.

diversity, which may be related to the different genetic backgrounds of HdrR and HNI (39). The combined heterogeneity of the complex interaction and stability of tetramer receptors is shown in Sissy (derived from partial recovery of *gsdf*-transgenic expression in *gsdf* KO), which led to the simultaneous entry of undifferentiated germ cells into oogenesis or spermatogenesis (Fig. 2*D*). Ovotestes were rare in *hotei* mutants (10%) but completely normal in Sissy (100%). This may reflect that the larger proportion of germ cells at early stage being more sensitive to Gsdf relative to Amh; in other words, most of the primordial oocytes are responsive to Gsdf but unresponsive to Amh. WB analysis showed that contrary to strong signal for anti-Smad1/5-P antibody in the normal XX ovary, the signal was not detected in the *gsdf* KO ovary (Fig. 8*A*). However, Amh in the *gsdf* KO was as high as that in the normal XY testis, which was much higher than that in the normal XX ovary (data not shown). Amh appears not to be required for triggering quiescent germ cells to proliferation in medaka (17). In addition, full-length AMH is less potent than C-terminal and cleaved AMH in stimulating Smad phosphorylation (40), suggesting the requirement of AMH processing for receptor engagement and Smad stimulation. Mechanisms subserving the Smad-independent pathway, however, cannot be excluded in early gametogenesis of medaka and requires further investigation.

Although there was no significant difference in the number of mitochondria between *gsdf* KO spermatogonia and normal XY spermatogonia, the abnormal morphology of *gsdf* KO mitochondria was obvious, which may be due to the damage caused by Gsdf and acyl-CoA interaction. In turn, this damage may induce ATP energy metabolism defects, and/or changes in cytoplasmic pH, and further influence protein synthesis and mitochondrial activity, which balanced germ cell proliferation and differentiation. In fact, the distal proximal disorder of the giant testes of gsdf KO XY^{HNI} is reminiscent of overproliferative "stem cysts," reflecting the disordered response of Gsdf signaling, which regulates the expansion of the cyst and/or delay in the normal progression of germ-cell differentiation. Tgfβ receptor II (*tgfbr2*) was only expressed in mouse quiescent gonocytes, which directly regulates the duration of quiescence (41).

In summary, our data provide a new insight into gametogenesis under the control of Gsdf and supermultifunctional eEF1α complexes. We show that the Gsdf–eEF1α appears necessary in the testes to balance undifferentiated and differentiated germ cells but is not sufficient to specify the male or female fate of germ cells. Further study on the mechanism of the expression shift between eEF1α and 42Sp50 under Gsdf regulation will facilitate a better understanding of the fundamental mechanisms of germ-cell proliferation, mitotic division, and differentiation at various levels, including chromosomal dynamics, DNA replication, and the RNA metabolism cascade.

DATA AVAILABILITY

The data set analyzed here has been deposited in ProteomeXchange with identifier PXD022153. All data are available in the associated supplementary data files.

Acknowledgments—We also thank ACCDON, LLC (www.accdon.com) for language-editing services, the National BioResource Project medaka for providing the HdrR and HNI strains as well as dmy mutant MT206 fish, Jingjie PTM Biolab Co, Ltd for assistance with proteomic analysis, and the Shanghai Institute of Biochemistry and Cell Biology for assistance with transmission electron microscope observations.

Funding and additional information—This work was supported by the First Class Discipline Program for Fishery from the Shanghai municipal government, a grant of the National Natural Science Foundation of China (81771545), and a grant of the National Key Research and Development Program of China 2018YFD0900601.

Author contributions—G. G., L. C., and Xiaomiao Zhao designed the experiments; methodologic investigations were performed by G. G., Xinting Zhang, Y. C., W. Z., F. Q., Y. Z., S. X., H. G., and Xiaozhu Zhong; writing, review, and editing was undertaken by G. G., Xinting Zhang, and Y. C.; and G. G., C. L., and Xiaomiao Zhao performed funding acquisition. All authors read and approved the final manuscript.

Conflict of interest—G. G. and S. X. declare their patent application for the method of Sissy medaka establishment (CN201811346983.9). All authors declare that they have no other conflicts of interest with the contents of this article.

Abbreviations—The abbreviations used are: amhr2, anti–Müllerian hormone receptor 2; DEPs, differentially expressed proteins; dlc1, dynein light chain 1; eEF1α, eukaryotic polypeptide elongation factor 1 alpha; *gsdf*, gonadal soma–derived factor; *KEGG*, kyoto encyclopedia of genes and genome; SMC3, structural maintenance of chromosomes 3; TGFβ, transforming growth factor β; WB, Western-blotted; Y2H, yeast 2-hybrid.

Received August 28, 2020, and in revised from, November 25, 2020 Published, MCPRO Papers in Press, December 8, 2020, https://doi.org/10.1074/mcp.RA120.002306

REFERENCES

1. Young, J. C., Wakitani, S., and Loveland, K. L. (2015) TGF-beta superfamily signaling in testis formation and early male germline development. *Semin. Cell Dev. Biol.* **45**, 94–103
2. Wang, Z. P., Mu, X. Y., Guo, M., Wang, Y. J., Teng, Z., Mao, G. P., Niu, W. B., Feng, L. Z., Zhao, L. H., and Xia, G. L. (2014) Transforming growth factor-beta signaling participates in the maintenance of the primordial follicle pool in the mouse ovary. *J. Biol. Chem.* **289**, 8299–8311
3. Shivdasani, A. A., and Ingham, P. W. (2003) Regulation of stem cell maintenance and transit amplifying cell proliferation by tgf-beta signaling in Drosophila spermatogenesis. *Curr. Biol.* **13**, 2065–2072
4. Foghi, A., Teerds, K. J., van der Donk, H., Moore, N. C., and Dorrington, J. (1998) Induction of apoptosis in thecal/interstitial cells: Action of transforming growth factor (TGF) alpha plus TGF beta on bcl-2 and interleukin-1 beta-converting enzyme. *J. Endocrinol.* **157**, 489–494
5. Foghi, A., Teerds, K. J., van der Donk, H., and Dorrington, J. (1997) Induction of apoptosis in rat thecal/interstitial cells by transforming growth factor alpha plus transforming growth factor beta *in vitro*. *J. Endocrinol.* **153**, 169–178
6. Sawatari, E., Shikina, S., Takeuchi, T., and Yoshizaki, G. (2007) A novel transforming growth factor-beta superfamily member expressed in gonadal somatic cells enhances primordial germ cell and spermatogonial proliferation in rainbow trout (Oncorhynchus mykiss). *Dev. Biol.* **301**, 266–275
7. Yan, Y. L., Desvignes, T., Bremiller, R., Wilson, C., Dillon, D., High, S., Draper, B., Buck, C. L., and Postlethwait, J. (2017) Gonadal soma controls ovarian follicle proliferation through Gsdf in zebrafish. *Dev. Dyn.* **246**, 925–945
8. Zhang, X., Guan, G. J., Li, M. Y., Zhu, F., Liu, Q. Z., Naruse, K., Herpin, A., Nagahama, Y., Li, J. L., and Hong, Y. H. (2016) Autosomal gsdf acts as a male sex initiator in the fish medaka. *Sci. Rep.* **6**, 19738
9. Jiang, D. N., Yang, H. H., Li, M. H., Shi, H. J., Zhang, X. B., and Wang, D. S. (2016) Gsdf is a downstream gene of dmrt1 that functions in the male sex determination pathway of the Nile tilapia. *Mol. Reprod. Dev.* **83**, 497–508
10. Imai, T., Saino, K., and Matsuda, M. (2015) Mutation of Gonadal soma-derived factor induces medaka XY gonads to undergo ovarian development. *Biochem. Biophys. Res. Commun.* **467**, 109–114
11. Nanda, I., Kondo, M., Hornung, U., Asakawa, S., Winkler, C., Shimizu, A., Shan, Z., Haaf, T., Shimizu, N., Shima, A., Schmid, M., and Schartl, M. (2002) A duplicated copy of DMRT1 in the sex-determining region of the Y chromosome of the medaka, Oryzias latipes. *Proc. Natl. Acad. Sci. U. S. A.* **99**, 11778–11783
12. Matsuda, M., Nagahama, Y., Shinomiya, A., Sato, T., Matsuda, C., Kobayashi, T., Morrey, C. E., Shibata, N., Asakawa, S., Shimizu, N., Hori, H., Hamaguchi, S., and Sakaizumi, M. (2002) DMY is a Y-specific DM-domain gene required for male development in the medaka fish. *Nature* **417**, 559–563
13. Nishimura, T., Sato, T., Yamamoto, Y., Watakabe, I., Ohkawa, Y., Suyama, M., Kobayashi, S., and Tanaka, M. (2015) Sex determination. foxl3 is a germ cell-intrinsic factor involved in sperm-egg fate decision in medaka. *Science* **349**, 328–331
14. Nishimura, T., Herpin, A., Kimura, T., Hara, I., Kawasaki, T., Nakamura, S., Yamamoto, Y., Saito, T. L., Yoshimura, J., Morishita, S., Tsukahara, T., Kobayashi, S., Naruse, K., Shigenobu, S., Sakai, N., *et al*. (2014) Analysis of a novel gene, Sdgc, reveals sex chromosome-dependent differences of medaka germ cells prior to gonad formation. *Development* **141**, 3363–3369
15. Nishimura, T., Yamada, K., Fujimori, C., Kikuchi, M., Kawasaki, T., Siegfried, K. R., Sakai, N., and Tanaka, M. (2018) Germ cells in the teleost fish medaka have an inherent feminizing effect. *PLoS Genet.* **14**, e1007259
16. Wu, X., Zhang, Y., Xu, S., Chang, Y., Ye, Y., Guo, A., Kang, Y., Guo, H., Xu, H., Chen, L., Zhao, X., and Guan, G. (2019) Loss of Gsdf leads to a dysregulation of Igf2bp3-mediated oocyte development in medaka. *Gen. Comp. Endocrinol.* **277**, 122–129
17. Nakamura, S., Watakabe, I., Nishimura, T., Picard, J. Y., Toyoda, A., Taniguchi, Y., di Clemente, N., and Tanaka, M. (2012) Hyperproliferation of mitotically active germ cells due to defective anti-Mullerian hormone signaling mediates sex reversal in medaka. *Development* **139**, 2283–2287

18. Morinaga, C., Saito, D., Nakamura, S., Sasaki, T., Asakawa, S., Shimizu, N., Mitani, H., Furutani-Seiki, M., Tanaka, M., and Kondoh, H. (2007) The hotei mutation of medaka in the anti-mullerian hormone receptor causes the dysregulation of germ cell and sexual development. *Proc. Natl. Acad. Sci. U. S. A.* **104**, 9691–9696
19. Vopalensky, P., Ruzickova, J., Pavlu, B., and Kozmik, Z. (2010) A lens-specific co-injection marker for medaka transgenesis. *Biotechniques* **48**, 235–236
20. Sun, K., Fan, L., Wang, C., Yang, X., Zhu, S., Zhang, X., Chen, X., Hong, Y., and Guan, G. (2017) Loss of gonadal soma derived factor damaging the pituitary-gonadal axis in medaka. *Sci. Bull.* **62**, 159–161
21. Xu, Q., Li, G., Cao, L., Wang, Z., Ye, H., Chen, X., Yang, X., Wang, Y., and Chen, L. (2012) Proteomic characterization and evolutionary analyses of zona pellucida domain-containing proteins in the egg coat of the cephalochordate, Branchiostoma belcheri. *BMC Evol. Biol.* **12**, 239
22. Wong, J. H., Alfatah, M., Sin, M. F., Sim, H. M., Verma, C. S., Lane, D. P., and Arumugam, P. (2017) A yeast two-hybrid system for the screening and characterization of small-molecule inhibitors of protein-protein interactions identifies a novel putative Mdm2-binding site in p53. *BMC Biol.* **15**, 108
23. Shu, F., Lv, S., Qin, Y., Ma, X., Wang, X., Peng, X., Luo, Y., Xu, B. E., Sun, X., and Wu, J. (2007) Functional characterization of human PFTK1 as a cyclin-dependent kinase. *Proc. Natl. Acad. Sci. U. S. A.* **104**, 9248–9253
24. Otake, H., Shinomiya, A., Matsuda, M., Hamaguchi, S., and Sakaizumi, M. (2006) Wild-derived XY sex-reversal mutants in the Medaka, Oryzias latipes. *Genetics* **173**, 2083–2090
25. Schneider, H., Dabauvalle, M. C., Wilken, N., and Scheer, U. (2010) Visualizing protein interactions involved in the formation of the 42S RNP storage particle of Xenopus oocytes. *Biol. Cell* **102**, 469–478
26. Kinoshita, M., Okamoto, G., Hirata, T., Shinomiya, A., Kobayashi, T., Kubo, Y., Hori, H., and Kanamori, A. (2009) Transgenic medaka enables easy oocytes detection in live fish. *Mol. Reprod. Dev.* **76**, 202–207
27. Macdonald, L. D., Knox, A., and Hansen, D. (2008) Proteasomal regulation of the proliferation vs. meiotic entry decision in the Caenorhabditis elegans germ line. *Genetics* **180**, 905–920
28. Lyons, S. M., Ricciardi, A. S., Guo, A. Y., Kambach, C., and Marzluff, W. F. (2014) The C-terminal extension of Lsm4 interacts directly with the 3' end of the histone mRNP and is required for efficient histone mRNA degradation. *RNA* **20**, 88–102
29. Joti, P., Ghosh-Roy, A., and Ray, K. (2011) Dynein light chain 1 functions in somatic cyst cells regulate spermatogonial divisions in Drosophila. *Sci. Rep.* **1**, 173
30. Miles, D. C., Wakeling, S. I., Stringer, J. M., van den Bergen, J. A., Wilhelm, D., Sinclair, A. H., and Western, P. S. (2013) Signaling through the TGF beta-activin receptors ALK4/5/7 regulates testis formation and male germ cell development. *PLoS One* **8**, e54606
31. Indu, S., Sekhar, S. C., Sengottaiyan, J., Kumar, A., Pillai, S. M., Laloraya, M., and Kumar, P. G. (2015) Aberrant expression of dynein light chain 1 (DYNLT1) is associated with human male factor infertility. *Mol. Cell. Proteomics* **14**, 3185–3195
32. Oulhen, N., Swartz, S. Z., Laird, J., Mascaro, A., and Wessel, G. M. (2017) Transient translational quiescence in primordial germ cells. *Development* **144**, 1201–1210
33. Mateyak, M. K., and Kinzy, T. G. (2010) eEF1A: Thinking outside the ribosome. *J. Biol. Chem.* **285**, 21209–21213
34. Kinoshita, M., Kani, S., Ozato, K., and Wakamatsu, Y. (2000) Activity of the medaka translation elongation factor 1alpha-A promoter examined using the GFP gene as a reporter. *Dev. Growth Differ.* **42**, 469–478
35. Kanamori, A. (2000) Systematic identification of genes expressed during early oogenesis in medaka. *Mol. Reprod. Dev.* **55**, 31–36
36. Kato, Y., Iwamori, T., Ninomiya, Y., Kohda, T., Miyashita, J., Sato, M., and Saga, Y. (2019) ELAVL2-directed RNA regulatory network drives the formation of quiescent primordial follicles. *EMBO Rep.* **20**, e48251
37. Guan, G., Sun, K., Zhang, X., Zhao, X., Li, M., Yan, Y., Wang, Y., Chen, J., Yi, M., and Hong, Y. (2017) Developmental tracing of oocyte development in gonadal soma-derived factor deficiency medaka (Oryzias latipes) using a transgenic approach. *Mech. Dev.* **143**, 53–61
38. Derynck, R., and Zhang, Y. E. (2003) Smad-dependent and Smad-independent pathways in TGF-beta family signalling. *Nature* **425**, 577–584
39. Horie, Y., Myosho, T., Sato, T., Sakaizumi, M., Hamaguchi, S., and Kobayashi, T. (2016) Androgen induces gonadal soma-derived factor, Gsdf, in XX gonads correlated to sex-reversal but not Dmrt1 directly, in the teleost fish, northern medaka (Oryzias sakaizumii). *Mol. Cell Endocrinol.* **436**, 141–149
40. di Clemente, N., Jamin, S. P., Lugovskoy, A., Carmillo, P., Ehrenfels, C., Picard, J. Y., Whitty, A., Josso, N., Pepinsky, R. B., and Cate, R. L. (2010) Processing of anti-mullerian hormone regulates receptor activation by a mechanism distinct from TGF-beta. *Mol. Endocrinol.* **24**, 2193–2206
41. Moreno, S. G., Attali, M., Allemand, I., Messiaen, S., Fouchet, P., Coffigny, H., Romeo, P. H., and Habert, R. (2010) TGFbeta signaling in male germ cells regulates gonocyte quiescence and fertility in mice. *Dev. Biol.* **342**, 74–84